Contribution from the Departments of Chemistry, Case Institute of Technology, Case Western Reserve University, Cleveland, Ohio 44106, and University of Edinburgh, Edinburgh, EH9 3JJ Scotland

Phosphine Adducts of Palladium(II) and Platinum(II) 1,1-Dithiolates. Single-Crystal X-ray Structures of Bis(diethyldithiocarbamato)(triphenylphosphine)platinum(II), $Pt(S_2CNEt_2)_2PPh_3$, Bis(diphenylphosphinodithioato)(triphenylphosphine)palladium(II), $Pd(S_2PPh_2)_2PPh_3$, Bis(*O*,*O*-diethyl dithiophosphato)(triphenylphosphine)platinum(II), $Pt(S_2P(OEt)_2)_2PPh_3$, and (Diphenylphosphinodithioato)bis(triethylphosphine)palladium(II) Diphenylphosphinodithioate, $[Pd(S_2PPh_2)(PEt_3)_2]S_2PPh_2$. Solution ^{31}P NMR Studies of the Dithiophosphate Complexes

JOHN P. FACKLER, JR.,*[1a] L. D. THOMPSON,[1a] IVAN J. B. LIN,[1a] T. ANTHONY STEPHENSON,[1b] ROBERT O. GOULD,[1b] JANET M. C. ALISON,[1b] and ALAN J. F. FRASER[1b]

Received October 20, 1981

Phosphine adducts of nickel triad 1,1-dithiolates are known to be fluxional. Four distinct structure types are known with coordination geometries MS_4P, MS_3P, and MS_2P_2, the latter containing either two dangling chelates or a bidentate chelate ligand and a noncoordinated thiolate anion. In this paper the X-ray crystal structures of $Pt(S_2CNEt_2)_2PPh_3$, $Pd(S_2PPh_2)_2PPh_3$, $Pt(S_2P(OEt)_2)_2PPh_3$, and $[Pd(S_2PPh_2)(PET_3)_2]S_2PPh_2$ are described. Dynamic NMR data implicate the formation of five-coordinate intermediates in the rearrangements of these complexes. The activation energy for rearrangement of the palladium(II) dithiophosphate complex is 7.8 kcal/mol while for the analogous platinum(II) complex it is 12.4 kcal/mol.

Introduction

Previous studies[2-8] have demonstrated that phosphines react with palladium(II) and platinum(II) dithiolates to rupture M–S bonds. The 1:1 phosphine complex generally shows a MS_3P coordination and contains both unidentate and bidentate dithiolate ligands (I). With additional tertiary phosphine,

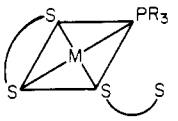

I

several reactions occur depending on the type of dithiolate, the solvent, and the steric properties of the ligands. With xanthates, $M(S_2COR)_2$, and dithiophosphates, $M(S_2P(OR)_2)_2$, C–O bond rupture can occur[2b,3a,4] to produce neutral species such as II or III, respectively. Esters of the dithiolate ligand

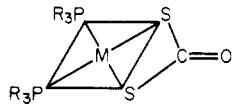

II

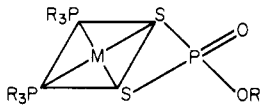

III

also are produced. With some tertiary phosphines, an anionic dithiolate ligand can be split off, leaving IV. However, so-

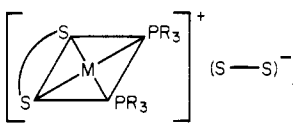

IV

lution and structural solid-state evidence also exists for the neutral trans species, V, a possible precursor to the ionic product, IV. In solution at room temperature these species are dynamic on the NMR time scale.[2a,3,5]

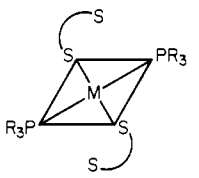

V

A reasonable understanding of the reaction chemistry of Pd(II) and Pt(II) dithiolates with phosphines now has emerged. This paper describes the detailed structural evidence for I with $Pt(S_2CNEt_2)_2PPh_3$ (obtained independently in each of our laboratories), $Pt(S_2P(OEt_2)_2)_2PPh_3$, and $Pd(S_2PPh_2)_2PPh_3$. The structure of an ionic bis(phosphine) product, $[Pd(S_2PPh_2)(PEt_3)_2]S_2PPh_2$(IV), also is described. Dynamic ^{31}P NMR studies of the species $M(S_2P(OEt)_2)_2PPh_3$, M = Pd(II), Pt(II), are presented and shown to be consistent with these structural results.

Experimental Section

Sample Preparations. Bright yellow crystals of bis(*N*,*N*-diethyldithiocarbamato)(triphenylphosphine)platinum(II) used for the X-ray structural study were prepared as reported.[3] The $Pd(S_2PPh_2)_2PPh_3$ was recrystallized from a CH_3NO_2/Et_2O mixture. Other monophosphine adducts were prepared by mixing the metal complexes with an equal molar ratio of the phosphine in solution. The $Pd(S_2PPh_2)_2(PEt_3)_2$ was recrystallized from CH_2Cl_2. Solution concentrations used for NMR experiments are $\sim 10^{-1}$ M. The carbon-13-enriched compound was prepared as described.[2b] Compounds involving phosphines (except triphenylphosphine) were handled under nitrogen atomosphere.

Instrumentation. The ^{13}C and ^{31}P NMR data reported in this work were obtained on a Varian XL-100 spectrometer operated at 25.16 and 40.5 MHz, respectively, in the Fourier transform mode. All ^{13}C chemical shifts are referenced downfield in ppm from the Me_4Si signal. The ^{31}P chemical shifts are referenced in ppm from 85% aqueous phosphoric acid. Upfield chemical shifts are recorded as positive. For variable-temperature studies the temperature was regulated with a Varian Model 604 controller. The temperatures were calibrated with a methanol standard.

The spin–lattice relaxation time of ^{31}P in $Pt(S_2P(OEt)_2)_2PPh_3$ was obtained with use of the Freeman–Hill inversion-recovery method.[9]

(1) (a) Case Western Reserve University. (b) University of Edinburgh.
(2) (a) J. P. Fackler, Jr., and W.-H. Pan, *J. Am. Chem. Soc.*, **101**, 1607 (1979); (b) I. J. B. Lin, H. W. Chen, and J. P. Fackler, Jr., *Inorg. Chem.*, **17**, 394 (1978), and references therein.
(3) (a) J. M. C. Alison and T. A. Stephenson, *J. Chem. Soc., Dalton Trans.*, 254 (1973); (b) D. F. Steele and T. A. Stephenson, *ibid.*, 2124 (1973).
(4) J. P. Fackler, Jr., J. A. Fetchin, and W. C. Seidel, *J. Am. Chem. Soc.*, **91**, 1217 (1969).
(5) J. M. C. Alison, T. A. Stephenson, and R. O. Gould, *J. Chem. Soc. A*, 3690 (1971).
(6) Other references can be found in recent reviews.[7,8]
(7) D. Coucouvanis, *Prog. Inorg. Chem.*, **26**, 302 (1979).
(8) R. P. Burns, F. P. McCullough, and C. A. McAuliffe, *Adv. Inorg. Chem. Radiochem.*, **23**, 211 (1980).

0020-1669/82/1321-2397$01.25/0

Table I. Crystal Data for $Pt(S_2CNEt_2)_2PPh_3$, $Pd(S_2PPh_2)_2PPh_3$, $Pt(S_2(OEt)_2)_2PPh_3$, and $[Pd(S_2PPh_2)(PEt_3)_2]S_2PPh_2$

	$Pt(S_2CNEt_2)PPh_3$[a]		$Pd(S_2PPh_2)_2PPh_3$	$Pt(S_2P(OEt)_2)_2PPh_3$	$[Pd(S_2PPh_2)(PEt_3)_2]S_2PPh_2$
cryst syst	monoclinic	monoclinic	triclinic	triclinic	monoclinic
space group	$P2_1/n$	$P2_1/c$	$B\bar{1}$	$P\bar{1}$	$C2/c$
a, Å	18.653 (4)	16.192 (4)	9.684 (30)	12.291 (9)	33.63 (4)
b, Å	9.9625 (69)	9.990 (3)	18.592 (30)	13.064 (8)	8.71 (2)
c, Å	16.1517 (58)	24.771 (5)	22.145 (30)	13.679 (6)	32.30 (5)
α, deg	90	90	90.576 (60)	113.06 (4)	90
β, deg	90.22 (2)	131.05 (1)	90.305 (60)	100.71 (5)	121.4 (1)
γ, deg	90	90	92.497 (60)	114.72 (5)	90
vol, Å^3	3001.4	3021	3983.2	1667.1	8075
Z	4	4	4	2	8
ρ(calcd), g/cm^3	1.67	1.66	1.45	1.65	1.38
ρ(measd), g/cm^3	1.65	1.66	1.43	1.65	1.3
no. of unique reflctns	3883	2602	2630	1985	1696
radiation	Cu Kα	Mo Kα_1	Cu Kα	Mo Kα_1	Cu Kα
μ, cm^{-1}	121.43	31.50	70.79	48.46	73.2

[a] First-column results from Edinburgh; second-column results from CWRU.

Collection and Reduction of X-ray Data. The structural results for $Pt(S_2CNEt_2)_2PPh_3$ obtained in Edinburgh were achieved[10] with Ni-filtered Cu Kα', λ = 1.5418 Å, radiation by using equiinclination Weissenberg photographs of a crystal oscillating about b. A total of 3392 independent reflections out to 2θ = 169.9° were obtained. A second crystal mounted along c allowed 491 additional planes to be collected. Intensities were estimated with a SAAB scanner linked to a PDP-15 computer. The data were corrected for Lorentz and polarization effects. The first crystal was corrected for absorption with a cylindrical approximation (0.4 × 0.16 × 0.32 mm crystal). The second crystal resembled a sphere of 0.15 mm and was corrected accordingly. Absences ($0k0$, $k = 2n + 1$; $h0l$, $h + l = 2n + 1$) suggested the space group $P2_1/n$ (alternative setting of $P2_1/c$, No. 14). Data for $Pt(S_2CNEt_2)_2PPh_3$, obtained at CWRU, were[11] from a crystal of approximate dimensions 0.30 × 0.25 × 0.20 mm on a Syntex $P2_1$ diffractometer using Mo Kα (λ = 0.710669 Å) radiation with variable-rate, 2θ–θ scans. Monochromatic data over the range $0° < 2\theta < 45°$ were corrected for Lorentz and polarization effects. No absorption correction was applied. 2602 reflections were obtained with $I > 3\sigma(I)$. A total of 15 well-centered reflections, $2\theta \approx 15$–30°, were used to obtain cell constants. Crystal data are collected in Table I.

Preliminary Weissenberg photographs[10] with Cu Kα radiation indicated that $Pd(S_2PPh_2)_2PPh_3$ forms triclinic crystals. Absences for reflections $h + l = 2n + 1$ indicated B centering for a nearly orthogonal cell, and the structure was solved in the space group $B\bar{1}$ (alternative setting for $P\bar{1}$, No. 2). A small needle-shaped crystal was used to obtain equiinclination Weissenberg photographs out to 2θ = 135°. The film data (Table I) were treated as described above.

Data for $Pt(S_2P(OEt)_2)_2PPh_3$ were obtained on a crystal 0.31 × 0.12 × 0.25 mm over the range $0 \le 2\theta \le 45°$ on a Syntex $P2_1$ diffractometer using monochromatic MoKα (λ = 0.7169 Å) radiation. With a 2θ–θ scan, 1985 reflections with $I \ge 3\sigma(I)$ were obtained for the triclinic crystal. No absorption corrections were made. Cell constants are presented in Table I.

An oscillation photograph produced the b-axis dimension for a small needlelike crystal of $Pd(S_2PPh_2)_2(PEt_3)_2$. Cell dimensions were obtained and refined from zero-level Weissenberg photographs: a = 33.63 (4) Å, b = 8.71 (2) Å, c = 32.30 (5) Å, β = 121.4 (1)°. Film data with Cu Kα radiation were treated as described above (Table I).

Refinement of Structures. Bis(diethyldithiocarbamato)(triphenylphosphine)platinum(II), $Pt(S_2CNEt_2)_2PPh_3$. The film data corrected for absorption (see above) were scaled. Several tests of the SAAB AFS MKS I automatic film scanner were made that indicated some inaccuracies in very weak and very high scanned intensities. Heavy-atom techniques and least-squares refinement gave R = 0.27 with the atom positions for PtS_4P. Successive difference Fourier maps led to the positions of the C and N atoms, which were refined isotropically to R = 0.11. After transformation of the coordinates by (101, 010, 100) this structure[10] is identical with that obtained more precisely from diffractometer data (Table II).

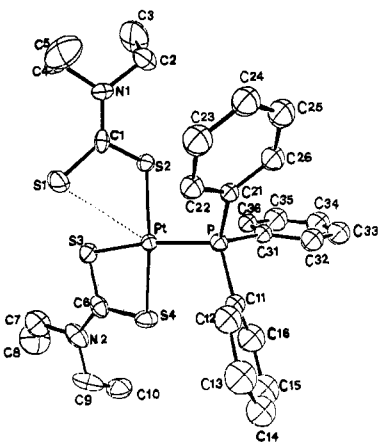

Figure 1. ORTEP drawing of $Pt(S_2CNEt_2)_2PPh_3$ at 40% probability for thermal ellipsoids.

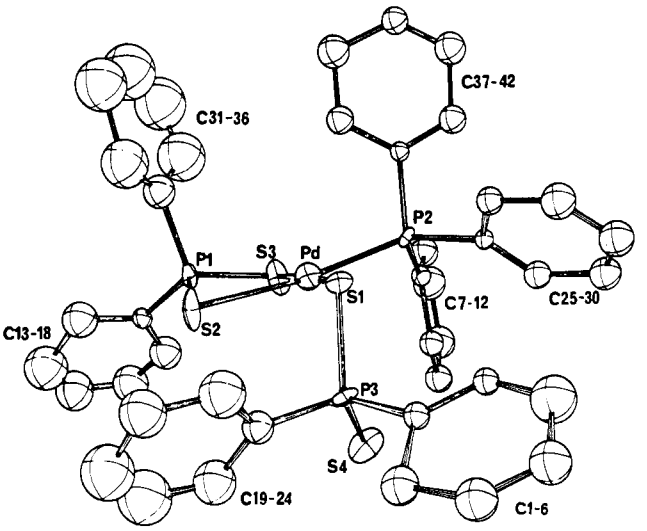

Figure 2. ORTEP drawing of $Pd(S_2PPh_2)_2PPh_3$.

The diffractometer data with anomolous dispersion and anisotropic refinement for Pt, S, and P gave R = 0.035 with R_w = 0.042 (with use of statistical weights). Thermal parameters are presented in Table S-I (supplementary material). An ORTEP drawing of the structure is given in Figure 1.

Bis(diphenylphosphinodithioato)(triphenylphosphine)palladium(II), $Pd(S_2PPh_3)_2PPh_3$. Heavy-atom positions obtained from Patterson methods were used for a difference Fourier map. Least-squares refinement for the heavy-atom (Pd, P, S, C) positions gave R = 0.20.

(9) R. Freeman and H. D. W. Hill, *Chem. Phys. Lett.*, **53**, 4103 (1970).
(10) For detail see J. M. C. Alison, Ph.D. Thesis, University of Edinburgh, 1973.
(11) For detail see I. J. B. Lin, Ph.D. Thesis, Case Western Reserve University, 1976.

Table II. Positional Parameters for $Pt(S_2CNEt_2)_2PPh_3$

atom	*x*	*y*	*z*
Pt	0.24843 (5)[a]	0.35851 (4)	0.50133 (3)
P	0.2238 (2)	0.2308 (3)	0.4170 (2)
S1	0.2965 (3)	0.1594 (4)	0.6336 (2)
S2	0.4193 (2)	0.2615 (3)	0.5898 (2)
S3	0.2546 (3)	0.5146 (4)	0.5756 (2)
S4	0.0907 (3)	0.4851 (4)	0.4251 (2)
C1	0.4040 (9)	0.1470 (13)	0.6374 (6)
N1	0.4846 (8)	0.0586 (10)	0.6781 (5)
C2	0.5695 (11)	0.0319 (15)	0.6724 (8)
C3	0.6763 (13)	0.1047 (22)	0.7313 (10)
C4	0.4894 (11)	−0.0298 (14)	0.7286 (7)
C5	0.4291 (13)	−0.1615 (17)	0.6930 (8)
C6	0.1294 (11)	0.5686 (13)	0.5003 (7)
N2	0.0668 (10)	0.6589 (12)	0.4979 (7)
C7	0.1023 (16)	0.7164 (18)	0.5664 (10)
C8	0.0856 (20)	0.8524 (23)	0.5647 (13)
C9	−0.0444 (11)	0.6927 (16)	0.4286 (10)
C10	−0.0356 (14)	0.8008 (19)	0.3883 (9)
C11	0.7867 (18)	0.2139 (11)	0.3363 (5)
C12	0.0164 (13)	0.1087 (16)	0.3276 (8)
C13	−0.0977 (14)	0.1024 (18)	0.2657 (9)
C14	−0.1439 (13)	0.2000 (17)	0.2145 (8)
C15	−0.0822 (14)	0.3081 (19)	0.2244 (9)
C16	0.0313 (14)	0.3177 (17)	0.2864 (9)
C21	0.2879 (9)	0.3048 (12)	0.3844 (6)
C22	0.2670 (11)	0.2509 (14)	0.3232 (7)
C23	0.3195 (12)	0.3166 (15)	0.3016 (8)
C24	0.3845 (12)	0.4271 (17)	0.3369 (8)
C25	0.4022 (13)	0.4807 (18)	0.3947 (7)
C26	0.3542 (10)	0.4153 (13)	0.4202 (6)
C31	0.2772 (9)	0.0594 (11)	0.4455 (6)
C32	0.3440 (10)	0.0013 (14)	0.4350 (7)
C33	0.3801 (11)	−0.1294 (15)	0.4580 (7)
C34	0.3505 (11)	−0.2038 (14)	0.4888 (7)
C35	0.2847 (11)	−0.1477 (16)	0.4994 (7)
C36	0.2461 (10)	−0.0135 (13)	0.4767 (6)

[a] Standard deviation in parentheses.

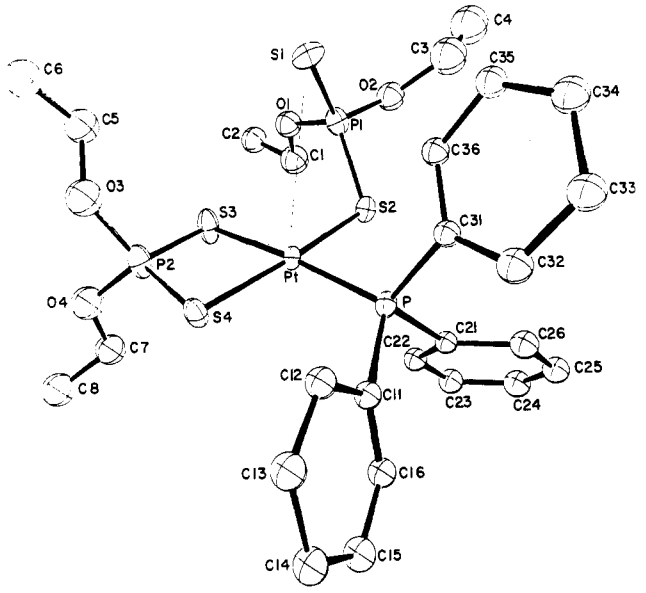

Figure 3. ORTEP drawing of $Pt(S_2P(OEt)_2)_2PPh_3$.

After correction for absorption and anisotropic refinement for Pd, P, and S, full-matrix least-squares refinement converged to $R = 0.112$. Fractional coordinates (Table III) and thermal parameters (Table S-III, supplementary material) are listed. Figure 2 is an ORTEP drawing.

Bis(*O*,*O*-diethyl dithiophosphato)(triphenylphosphine)platinum(II), $Pt(S_2P(OEt)_2)_2PPh_3$. Heavy-atom procedures led to the Pt, S, and P atom positions. R and R_w converged to 0.064 and 0.059 with use of anisotropic treatment for Pt, S, and P without producing well-defined thermal parameters for several of the C atoms. Since disorder or large thermal motions are likely for the ethyl groups and the electron density

Table III. Positional and Thermal Parameters for $Pd(S_2PPh_2)_2PPh_3$

Palladium, Sulfur, and Phosphorus Atoms

atom	*x*	*y*	*z*
Pd	0.2261 (2)	0.2562 (1)	0.0570 (1)
S1	0.0900 (8)	0.1762 (4)	−0.0021 (3)
S2	0.1228 (9)	0.3604 (4)	0.0145 (3)
S3	0.3588 (9)	0.3433 (4)	0.1138 (4)
S4	0.3878 (10)	0.2155 (4)	−0.0786 (4)
P1	0.2125 (8)	0.4094 (3)	0.0855 (3)
P2	0.3236 (7)	0.1701 (3)	0.1134 (3)
P3	0.1899 (8)	0.1875 (4)	−0.0829 (3)

Phenyl Carbon Atoms

atom	*x*	*y*	*z*	$100U$, Å^2
C1	0.1599 (30)	0.1008 (13)	−0.1195 (11)	2.1 (6)
C2	0.1247 (36)	0.1010 (16)	−0.1840 (14)	4.0 (8)
C3	0.1042 (41)	0.0244 (18)	−0.2074 (15)	4.8 (9)
C4	0.1346 (39)	−0.0333 (18)	−0.1791 (15)	4.7 (9)
C5	0.1800 (46)	−0.0266 (21)	−0.1168 (18)	6.1 (11)
C6	0.1945 (32)	0.0390 (14)	−0.0884 (12)	2.3 (7)
C7	0.3168 (29)	0.0754 (13)	0.0897 (11)	1.6 (6)
C8	0.4351 (35)	0.0381 (15)	0.0792 (13)	3.3 (7)
C9	0.4296 (37)	−0.0355 (16)	0.0652 (14)	3.9 (8)
C10	0.2990 (38)	−0.0693 (17)	0.0558 (14)	4.4 (8)
C11	0.1827 (39)	−0.0310 (16)	0.0649 (14)	4.3 (8)
C12	0.1855 (34)	0.0409 (14)	0.0822 (12)	2.8 (7)
C13	0.2819 (31)	0.4961 (14)	0.0704 (12)	2.3 (6)
C14	0.1913 (45)	0.5461 (20)	0.0537 (17)	6.2 (10)
C15	0.2700 (62)	0.6204 (26)	0.0316 (22)	9.1 (15)
C16	0.3985 (58)	0.6310 (25)	0.0372 (21)	7.5 (13)
C17	0.4757 (48)	0.5826 (21)	0.0584 (17)	6.6 (11)
C18	0.4266 (44)	0.5145 (20)	0.0729 (16)	5.9 (10)
C19	0.0967 (34)	0.2473 (15)	−0.1252 (13)	3.2 (7)
C20	−0.0486 (49)	0.2379 (22)	−0.1312 (18)	6.8 (12)
C21	−0.1318 (50)	0.2869 (22)	−0.1610 (18)	6.6 (12)
C22	−0.0494 (56)	0.3497 (24)	−0.1834 (20)	8.7 (13)
C23	0.0777 (80)	0.3588 (34)	−0.1776 (28)	10.1 (21)
C24	0.1610 (47)	0.3103 (21)	−0.1515 (17)	6.5 (10)
C25	0.4985 (29)	0.1939 (13)	0.1255 (11)	1.9 (6)
C26	0.5660 (37)	0.2097 (16)	0.1780 (14)	3.9 (8)
C27	0.6997 (49)	0.2329 (22)	0.1845 (18)	6.7 (11)
C28	0.7952 (46)	0.2380 (20)	0.1350 (17)	5.6 (11)
C29	0.7309 (40)	0.2213 (18)	0.0737 (15)	4.5 (9)
C30	0.5869 (33)	0.1973 (15)	0.0722 (15)	2.7 (7)
C31	0.0889 (43)	0.4222 (18)	0.1468 (16)	5.2 (9)
C32	−0.0515 (61)	0.4156 (26)	0.1303 (22)	9.1 (16)
C33	−0.1515 (76)	0.4254 (32)	0.1910 (28)	11.9 (21)
C34	−0.0645 (104)	0.4357 (41)	0.2442 (37)	14.3 (28)
C35	0.0656 (100)	0.4410 (40)	0.2546 (35)	15.1 (27)
C36	0.1343 (77)	0.4224 (33)	0.2048 (30)	11.8 (20)
C37	0.2440 (29)	0.1654 (13)	0.1864 (11)	1.8 (6)
C38	0.2774 (36)	0.1106 (16)	0.2246 (13)	3.6 (8)
C39	0.2002 (37)	0.0991 (16)	0.2828 (14)	4.2 (8)
C40	0.1039 (33)	0.1456 (15)	0.2936 (12)	3.1 (7)
C41	0.0689 (41)	0.2077 (18)	0.2576 (15)	4.8 (9)
C42	0.1501 (38)	0.2162 (16)	0.2033 (14)	3.7 (8)

associated with their positions has such a small influence on the structural model for the Pt, S, and P positions, refinement was terminated. Coordinates, Table IV, and thermal parameters, Table S-V (supplementary material), are presented. An ORTEP drawing of the structure is presented in Figure 3.

(Diphenylphosphinodithioato)bis(triethylphosphine)palladium(II) Diphenylphosphinodithioate, $[Pd(S_2PPh_2)(PEt_3)_2]S_2PPh_2$. Palladium atoms were located by Patterson methods. Fourier and difference Fourier maps located the rest of the non-H atoms. Final refinement allowed Pd and S to vary anisotropically, bringing R to convergence at 0.126. An ORTEP drawing of the structure is presented in Figure 4 with coordinates in Table V and thermal parameters in Table S-VII (supplementary material).

NMR Studies of $M(S_2P(OEt)_2)_2PPh_3$, M = Pd, Pt. The $^{31}P\{^1H\}$ NMR spectrum of $Pt(S_2P(OEt)_2)_2$ in $CDCl_3$ shows a 1:4:1 triplet at −101.0 ppm. The triplet is due to the coupling between ^{31}P and ^{195}Pt (^2J = 445 Hz) in which the ^{195}Pt has natural abundance 33% and nuclear spin $I = {}^1/_2$.

Table IV. Positional Parameters for $Pt(S_2P(OEt)_2)_2PPh_3$

atom	x	y	z	B, Å²
P	0.04961	0.48109	0.22603	
S1	0.43473	0.65887	0.39268	
S2	0.16615	0.41225	0.13104	
P1	0.35716	0.56365	0.22424	
S3	0.13694	0.68014	0.22241	
S4	−0.05894	0.56475	0.32255	
P2	0.04762	0.72869	0.32117	
O1	0.39114	0.67298	0.18847	8.89
C1	0.34215	0.63647	0.07414	12.32
C2	0.42214	0.76988	0.07269	10.91
O2	0.43433	0.49961	0.16666	9.78
C3	0.48357	0.43032	0.22014	14.76
C4	0.57277	0.42931	0.20277	16.65
O3	0.15293	0.85382	0.45664	10.94
C5	0.29690	0.94731	0.49373	10.55
C6	0.34634	1.03150	0.61557	11.70
O4	−0.02621	0.78780	0.29043	10.61
C7	−0.11850	0.72040	0.17858	9.73
C8	−0.20073	0.77222	0.17023	11.73
P	−0.04978	0.28789	0.21867	4.82
C11	−0.19696	0.24580	0.24814	4.82
C12	−0.17137	0.32487	0.37004	5.15
C13	−0.27845	0.30535	0.3994	5.75
C14	−0.40783	0.21263	0.30967	5.74
C15	−0.42708	0.13948	0.19381	5.99
C16	−0.32352	0.15757	0.16263	5.26
C21	0.05316	0.27066	0.31567	4.65
C22	−0.01216	0.17438	0.34770	6.55
C23	0.07257	0.15948	0.42159	6.26
C24	0.20914	0.23949	0.46572	6.32
C25	0.26751	0.33732	0.44127	5.52
C26	0.18846	0.35362	0.36601	5.06
C31	−0.11682	0.14584	0.07264	4.42
C32	−0.12338	0.02934	0.06120	6.39
C33	−0.17347	−0.07480	−0.06211	6.28
C34	−0.20486	−0.05760	−0.15003	7.58
C35	−0.19937	0.05680	−0.13768	6.85
C36	−0.14959	0.16161	−0.02017	5.58

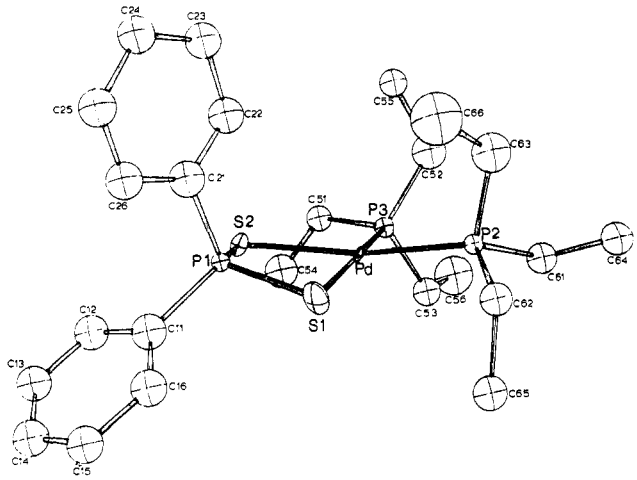

Figure 4. ORTEP drawing of $[Pd(S_2PPh_2)(PEt_3)_2]^+$.

The room-temperature $^{31}P\{^1H\}$ NMR spectrum of $Pt(S_2P(OEt)_2)_2$ in $CDCl_3$ in the presence of one PPh_3 molecule per Pt atom shows the dithiophosphate (DTP) region to be a triplet (1:4:1) of doublets (1:1) centered at −97.2 ppm. The phosphine is a triplet (1:4:1) of triplets (1:2:1) centered at −13.6 ppm. When the temperature is decreased from 31 to −48 °C, the triplet of doublets in the DTP region collapses and splits to a triplet (1:4:1) of doublets and a triplet (1:4:1) (Figure 5). The phosphine signal also changes to a triplet (1:4:1) of doublets (1:1). It is obvious that there are two magnetically nonequivalent dithiophosphate ligands at low temperature in $CDCl_3$. One of the DTP phosphorus atoms is coupled to the ^{195}Pt and the phosphine ^{31}P ($^2J_{P-Pt}$ = 120 and $^3J_{P-P}$ = 13 Hz). The other has $^2J_{P-Pt}$ = 336 and $^3J_{P-P}$ < 1 Hz. At room temperature the two DTP ligands appear equivalent. A similar behavior has been found[13b] in the variable-temperature $^{31}P\{^1H\}$ NMR studies of $Pt(S_2PPh_2)_2PMePh$.

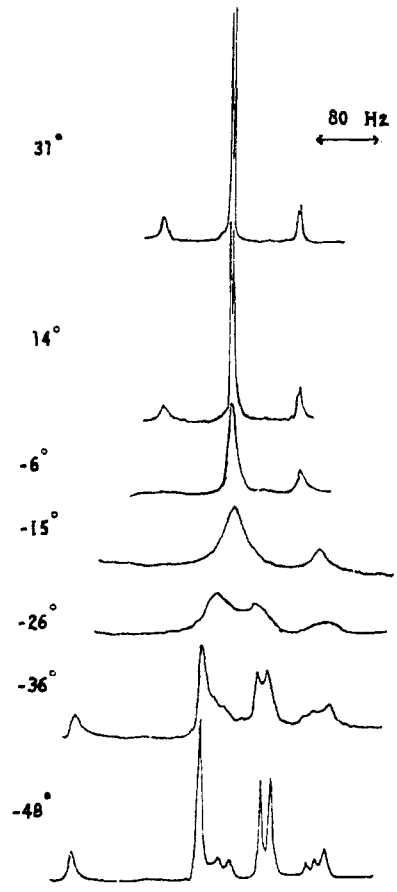

Figure 5. Proton-decoupled ^{31}P NMR spectra of $Pt(S_2P(OEt_2)_2PPh_3$ in $CDCl_3$ at different temperatures in the dithiophosphate region of the spectrum. Satellites due to ^{195}Pt coupling (~33%) are readily observed for each ligand P. Coupling to PPh is observed for only one of the dithiophosphate ligands at −48 °C.

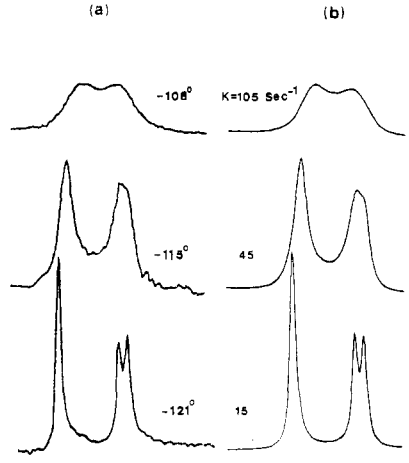

Figure 6. (a) Proton-decoupled ^{31}P NMR spectra in the dithiophosphate region of $Pd(S_2P(OEt)_2)_2PPh_3$ in a 2:3 mixture of acetone-d_6/diethyl ether at three temperatures. (b) Computer-simulated DNMR-3 spectra.

The palladium complex, $Pd(S_2P(OEt)_2)_2PPh_3$, exhibits dynamical behavior similar to that of its platinum analogue over the temperature range of −60 to −121 °C in a mixture of acetone-d_6 and diethyl ether (Figure 6). (At −121 °C there are two magnetically nonequivalent DTP ligands coupled to the phosphine ^{31}P $^3J_{P-P}$ = 12, <1 Hz, respectively.) At −60 °C the two DTP ligands become equivalent, giving a doublet for the DTP P atoms and a triplet for the phosphine P atom. From −60 to −20 °C the line shape remains unchanged. Above −20 °C, however, both the DTP doublets collapse to broad signals. Therefore, two distinct dynamical processes occur in the palladium complex, whereas only one process is observed for the corresponding

Table V. Fractional Coordinates of Atoms in $[Pd(S_2PPh_2)(PEt_3)_2]S_2PPh_2$

atom	x	y	z	U, Å²
		Palladium, Sulfur, and Phosphorus Atoms		
Pd	0.2183 (1)	0.0414 (3)	0.3195 (1)	
S1	0.1387 (4)	−0.0503 (15)	0.2831 (4)	
S2	0.1894 (4)	0.1273 (12)	0.2379 (4)	
S3	0.1790 (5)	0.0468 (24)	0.5001 (5)	
S4	0.1056 (5)	−0.1739 (12)	0.5154 (5)	
P1	0.1275 (4)	0.0742 (11)	0.2261 (4)	0.013 (3)
P2	0.2316 (4)	−0.0042 (10)	0.3965 (4)	0.015 (3)
P3	0.2935 (4)	0.1130 (12)	0.3453 (4)	0.018 (3)
P4	0.1157 (4)	−0.0146 (11)	0.4776 (4)	0.016 (3)
		Ethyl Carbon Atoms		
C51	0.2996	0.1835	0.2985	0.030
C52	0.3183	0.2663	0.3912	0.054
C53	0.3322	−0.0490	0.3671	0.036
C54	0.3015	0.0878	0.2601	0.053
C55	0.2859	0.4279	0.3739	0.033
C56	0.3867	−0.0142	0.3951	0.076
C61	0.2893	−0.0565	0.4460	0.036
C62	0.1921	−0.1361	0.3972	0.033
C63	0.2224	0.1680	0.4197	0.056
C64	0.2942	−0.0579	0.4972	0.039
C65	0.1968	−0.3200	0.3813	0.041
C66	0.1709	0.2405	0.3843	0.092
		Phenyl Carbon Atoms		
C11	0.0945	−0.0360	0.1706	0.042
C12	0.0970	−0.0026	0.1291	0.042
C13	0.0694	−0.0805	0.0857	0.042
C14	0.0388	−0.1934	0.0834	0.042
C15	0.0337	−0.2341	0.1214	0.042
C16	0.0623	−0.1541	0.1674	0.042
C21	0.0911	0.2371	0.2188	0.042
C22	0.1146	0.3516	0.2517	0.042
C23	0.0885	0.4887	0.2487	0.042
C24	0.0392	0.4971	0.2113	0.042
C25	0.0181	0.3721	0.1791	0.042
C26	0.0438	0.2427	0.1827	0.042
C31	0.0900	−0.0745	0.4145	0.042
C32	0.0706	0.0310	0.3755	0.042
C33	0.0522	−0.0182	0.3280	0.042
C34	0.0529	−0.1747	0.3190	0.042
C35	0.0707	−0.2856	0.3541	0.042
C36	0.0903	−0.2370	0.4043	0.042
C41	0.0781	0.1512	0.4693	0.042
C42	0.0347	0.1248	0.4619	0.042
C43	0.0068	0.2574	0.4583	0.042
C44	0.0261	0.4101	0.4626	0.042
C45	0.0714	0.4250	0.4702	0.042
C46	0.0974	0.2967	0.4736	0.042

platinum compound over the temperature range studied.

A computer-simulated line-shape analysis for the palladium complex (assuming an ABX spin system with A and B interchange) is presented in Figure 6. However, in the phosphine region, only the central peak of the 1:2:1 triplet changes, the two outer peaks remaining sharp. Exchange of the spin state of A and B does not affect the $\beta\beta\beta \rightarrow \beta\beta\alpha$ and $\alpha\alpha\beta \rightarrow \alpha\alpha\alpha$ transitions corresponding to the two outer lines.

An Arrhenius plot for exchange in the palladium compound gives an activation energy, E_a, of 7.8 kcal/mol if monodentate–bidentate ligand exchange is assumed. The $\Delta G^{\ddagger}$ value for the corresponding platinum compound calculated near the coalescence temperature (−27 °C) is 12.4 kcal/mol.

A phosphate ^{31}P spin–lattice relaxation study was performed on $Pt(S_2P(OEt)_2)_2PPh_3$ at −50 °C. The pulse sequence[12] of [... T...90°(S_∞...T...180°...t...90°(S_t)...)] gives spin–lattice relaxation times (T_1) calculated by using the relationship

$$\ln (S - S_t) = \ln (2S) - t/T_1$$

(12) S_∞ and S_t denote the resonance intensities of specific nuclei observed with a long waiting time and some chosen time interval between the 180 and 90° pulses. T represents the sum of pulse delay and pulse acquisition time.

Table VI. Selected Lengths (Å) and Angles (Deg) in $Pt(S_2CNEt_2)_2PPh_3$

	Bond Lengths about Metal Atom		
Pt-P	2.250 (4)	Pt-S3	2.365 (5)
Pt-S2	2.331 (3)	Pt-S4	2.313 (3)
	Bond Lengths for the Monodentate Ligand		
S1-C1	1.685 (19)	N1-C4	1.491 (22)
S2-C1	1.771 (17)	C2-C3	1.528 (21)
C1-N1	1.331 (14)	C4-C5	1.527 (21)
N1-C2	1.497 (27)		
	Bond Lengths for the Bidentate Ligand		
S3-C6	1.707 (11)	N2-C9	1.497 (16)
S4-C6	1.740 (18)	C7-C8	1.381 (30)
C6-N2	1.329 (25)	C9-C10	1.530 (33)
N2-C7	1.505 (31)		
	Bond Lengths for the Phosphine		
P-C11	1.838 (8)	C13-C14	1.368 (24)
P-C21	0.837 (19)	C23-C24	1.372 (21)
P-C31	1.838 (12)		
	Some Nonbonded Distances		
Pt-S1	3.457 (5)	S3-S4	2.835 (5)
S1-S2	3.000 (8)		
	Angles about the Metal Atom		
P-Pt-S2	90.8 (2)	S3-Pt-S4	74.6 (2)
S2-Pt-S3	97.2 (2)	S4-Pt-P	97.1 (2)

giving 2.2 s for both DTP ^{31}P nuclei.

NMR Studies of $Pt(S_2CNR_2)_2Pr'_3$. The ^{13}C NMR spectrum of $Pt(S_2CN(i\text{-}Bu)_2)_2PMe_2Ph$ in $CDCl_3$ at 0 °C shows α-, β-, γ-, and S_2CN carbon resonances located at 206.3, 59.6, 26.8, and 20.2 ppm, respectively. The α-, β-, and γ-carbon resonances are sharp singlets, while the S_2CN carbon signal is a 1:4:1 triplet due to the coupling of ^{13}C with ^{195}Pt ($^2J_{C-Pt}$ = 62 Hz). When the temperature is decreased to −51 °C, the α-carbon signal and the S_2CN triplet both broaden. At −60 °C, the α-carbon resonance splits to two broad signals and the S_2CN carbon resonance gives two unresolved signals. So that a lower temperature could be obtained, CH_2Cl_2 was added to the $CDCl_3$ solution. The spectrum at −70 °C shows two well-separated S_2CN carbon signals, a 1:4:1 triplet at δ 206.4 with $^2J_{C-Pt}$ = 56 Hz and a singlet at δ 203.0.

The $\Delta G^{\ddagger}$ value calculated from these data at −60 °C is 10.0 kcal/mol.

Discussion

Solution and solid-state structural data for phosphine adducts of nickel triad 1,1-dithiolates identify several different structural types. In addition to nonionic products, V, excess phosphine can produce ionic species[13] such as $[M(S\text{–}S)(PR'_3)_2]S_2PPh_2$ (M = Pd, Pt; S–S = $^-S_2CNR_2$, $^-S_2PR_2$) depending on the specific properties of the metal, the 1,1-dithiolate, the phosphine, and the solvent. The processes that lead to exchange in solution between the dithiolate ligands have been discussed.[2,3]

With equivalent amounts of added phosphine, 1:1 adducts are obtained with the dithiolates of Ni(II), Pd(II), and Pt(II). Although detailed structural results are limited, it is known[14] that $Ni(S_2P(OEt)_2)_2PPh_3$ contains an approximately square-pyramidal NiS_4P geometry in this paramagnetic product. All palladium(II) and platinum(II) complexes studied to date[15,17,21]

(13) (a) See J. A. Goodfellow, T. A. Stephenson, and M. C. Cornock, *J. Chem. Soc., Dalton Trans.*, 1195 (1978), and references therein; (b) M. C. Cornock and T. A. Stephenson, *ibid.*, 501 (1977).
(14) H. W. Chen, Ph.D. Thesis, Case Western Reserve University, 1977.
(15) In addition to the structures reported here, an incomplete X-ray structural study[16] for $Pt(S_2COEt)_2PPh_3$ shows the presence of a dangling dithiolate ligand. In this case, however, the noncoordinated atom closest to the Pt appears to be the O atom (at ~3.4 Å).
(16) L. D. Thompson and J. P. Fackler, Jr., unpublished results.
(17) D. R. Swift, Ph.D. Thesis, Case Western Reserve University, 1970.
(18) R. C. Elder, M. J. Heeg, D. Payne, M. Tricula, and E. Deutsch, *Inorg. Chem.*, **17**, 431 (1978).

Table VII. Selected Distances (Å) and Angles (Deg) for $Pd(S_2PPh_2)_2PPh_3$

	Bond Lengths about the Metal Atoms		
Pd-S2	2.416 (9)	Pd-S4	3.485 (11)
Pd-S3	2.369 (9)	Pd-P2	2.274 (8)
Pd-S1	2.331 (9)		
	Bond Lengths for the Monodentate Ligand		
S1-P3	2.047 (10)	P3-C1	1.808 (25)
S4-P3	1.966 (13)	P3-C19	1.740 (31)
	Bond Lengths for the Bidentate Ligand		
S2-P1	1.986 (11)	P1-C13	1.755 (27)
S3-P1	2.017 (12)	P1-C31	1.835 (39)
	Angles about the Metal Atom		
S2-Pd-S3	83.6 (3)	P2-Pd-S3	87.9 (3)
S2-Pd-S1	92.9 (3)	S2-Pd-P2	169.3 (2)
S1-Pd-P2	95.6 (3)	S1-Pd-S3	176.5 (4)
	Angle in the Monodentate Ligand		
	S1-P3-S4 116.3 (5)		
	Angle in the Bidentate Ligand		
	S2-P1-S3 105.7 (4)		

Table VIII. Selected Bond Lengths (Å) and Angles (Deg) of $Pt(S_2P(OEt)_2)_2PPh_3$

	Lengths		
Pt-S2	2.325 (10)	C1-C2	1.61 (7)
Pt-S3	2.388 (12)	O2-C3	1.59 (7)
Pt-S4	2.337 (11)	O2-C4	2.30 (8)
Pt-P	2.247 (9)	C3-C4	1.16 (9)
S1-P1	1.926 (12)	O3-C5	1.50 (4)
S2-P1	2.01 (10)	O3-C6	2.29 (3)
P1-O1	1.60 (3)	C5-C6	1.40 (5)
P1-O2	1.62 (3)	O4-C7	1.36 (4)
S3-P2	1.97 (2)	O4-C8	2.32 (5)
S4-P2	2.00 (1)	C7-C8	1.44 (7)
P2-O3	1.65 (2)	P-C11	1.83 (3)
P2-O4	1.51 (4)	P-C21	1.80 (3)
O1-C1	1.36 (5)	P-C31	1.82 (2)
O1-C2	2.37 (5)		
	Some Nonbonded Distances		
Pt-S1	3.95 (5)	S1-S2	3.429 (9)
Pt-P2	2.98 (1)	S3-S4	3.123 (16)
	Angles		
Pt-S2-P1	106.1 (6)	S3-Pt-S4	82.7 (3)
S2-Pt-S3	93.2 (5)	S2-Pt-P	88.7 (4)
Pt-S3-P2	85.9 (7)	S3-Pt-P	175.0 (5)
S2-Pt-S4	175.9 (5)	S4-Pt-P	95.3 (4)

display four-coordinate planar MS_3P geometries with a dangling dithiolate ligand.

In $Pt(S_2CNEt_2)_2PPh_3$ (Table VI) there are four distinct Pt–S distances, three within the normal range of 2.2–2.4 Å for bond formation. The Pt–S bond trans to the P atom (2.365 Å) clearly displays the trans influence or structural trans effect (STE)[18] of the phosphine. The Pt–S nonbonded distance in the dangling ligand (3.457 Å) is slightly longer than the nonbonded Pt–S distance (3.392 Å) in[2b] $Pt(S_2CN(i\text{-}Bu)_2)_2(PMe_2Ph)_2$. The C–N distances (1.331 and 1.329 Å) reflect partial double-bond character as normally found[7] with metal dithiocarbamates. It is interesting that the Pt atom is displaced slightly (~0.074 Å) above the PtS_3P plane toward the nonbonded S atom. As expected, the S···S "bite" distance is larger (3.000 (8) Å) in the monodentate ligand compared with that in the bidentate ligand (2.835 (5) Å).

In $Pd(S_2PPh_2)_2PPh_3$ four different metal–sulfur distances also are observed (Table VII) three within normal Pd–S bonding values of 2.2–2.5Å. The dangling ligand contains a 3.48 Å nonbonding Pd–S distance. This structure was inferred[5] from IR studies of the complex. Again a STE is observed with the longest Pd–S bond being trans to the phosphine. Deviations from planarity for the PdS_3P coordination geometry are less than 0.081 Å. In the formation of the dangling ligand, the S–P–S angle opens to 99.6 (4)° from 83° in the bidentate ligand. The S–S "bite" increases from 3.19 to 3.41 Å in the dangling ligand. Any interaction between the Pd and the dangling S atom is weak.

In $Pt(S_2P(OEt)_2)_2PPh_3$ the coordination geometry also is similar to that found in $Pt(S_2CNEt_2)_2PPh_3$. Three Pt–S distances (Table VIII) are bonding with the fourth (Pt–S_1 = 3.954 (5) Å) clearly nonbonding. A STE is observed here also

Table IX. Selected Bond Lengths (Å) and Angles (Deg) for $[Pd(S_2PPh_2)(PEt_3)_2]S_2PPh_2$

	Cation		
Pd-S1	2.429 (13)	Pd-P3	2.300 (14)
Pd-S2	2.405 (13)	S1-P1	1.996 (18)
Pd-P2	2.320 (15)	S2-P1	1.966 (20)
S1-Pd-S2	81.9 (4)	Pd-S1-P1	84.2 (6)
P2-Pd-P3	95.6 (5)	Pd-S2-P1	85.4 (7)
P2-Pd-S1	90.6 (5)	S1-P1-S2	106.1 (6)
P3-Pd-S2	93.0 (5)	C11-P1-C21	105.2 (5)
	Anion		
P4-S3	1.932 (20)	P4-S4	1.990 (20)
S3-P4-S4	117.9 (8)	C31-P4-C41	99.9 (4)

Scheme I. Reactions with Phosphines

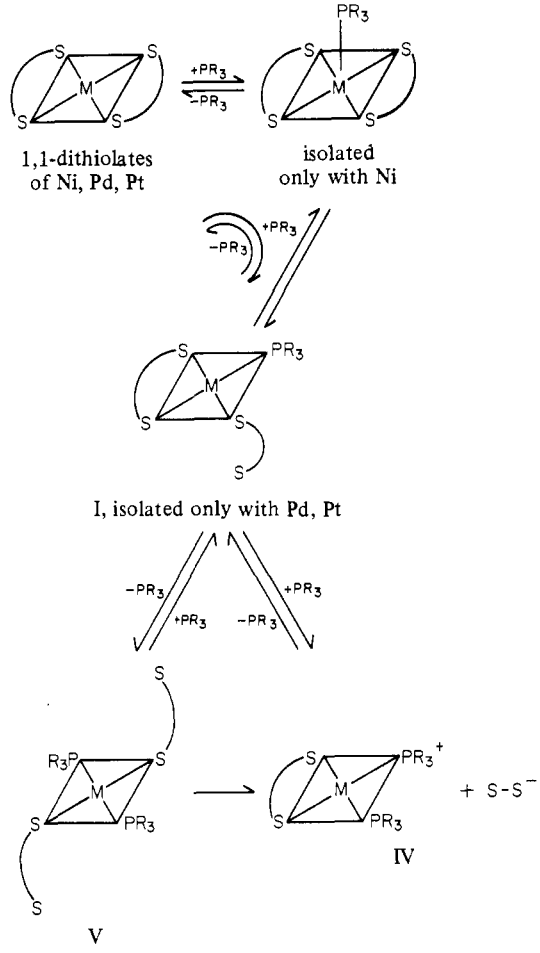

(19) P. Pregosin and R. W. Kunz, "^{31}P and ^{13}C NMR of Transition Metal Phosphine Complexes", Springer-Verlag, New York, 1979.
(20) Six-coordinate $Ni(S\text{–}S)_3^-$ anions also are obtained[7,8] with Ni(II) and excess anionic ligand.
(21) Similar observations concerning Pd(II) and Pt(II) coordination geometries have been made with chelating phosphines.[22] These complexes also are dynamic on the NMR time scale.
(22) D. W. Meek and T. J. Mazanec, *Acc. Chem. Res.*, **14**, 266 (1981).

with the trans-Pt–S distance ~0.05 Å longer than the cis-Pt–S distances. Since data to only $\theta \cong 22.5°$ were collected and disorder may exist in the ethoxy groups, further detailed discussion of the structural features appears unwarranted.

The structure of $[Pd(S_2PPh_2)(PEt_3)_2]S_2PPh_2$ is unambiguously that of a four-coordinate (PdS_2P_2) cation with a dithiolate anion. The Pd–S distances are equal to within two standard deviations (Table IX) for the bonded atoms and comparable to the trans-Pd–S distance in $Pd(S_2PPh_2)_2PPh_3$. Distances and angles generally are comparable in the two structures for similarly bonded atoms. The anionic ligand shows a S–P–S angle of 117.9 (8)°, only slightly larger than the 113.9 (10)° angle of the dangling ligand in $Pd(S_2PPh_2)_2PPh_3$.

In addition to evidence for each of the structures observed in the solid state for phosphine adducts of 1,1-dithiolate, phosphine exchange also occurs in solution. The ^{31}P NMR line shape observed for $Pd(S_2P(OEt)_2)_2PPh_3$ above −20 °C clearly shows this by loss of P–P coupling. Over the same temperature range this phosphine exchange is much slower with the Pt than with the analogous Pd complexes.

The activation energy $\Delta G^{\ddagger}$ of 12.4 kcal/mol at −27 °C is comparable with the ^1H results (12.5 kcal/mol) reported previously[3a] for uni-/bidentate $^-S_2P(OEt)_2$ ligand exchange in $Pt(S_2P(OEt)_2)_2PPh_3$. The fact that the apparent T_1 for both dithiophosphate P atoms is the same (and shorter than the lifetime for exchange) suggests that the equivalence is due to the exchange process and hence likely an intramolecular process. Intramolecular exchange has been established[2a] to be the process producing equivalent ligands in $Pt(Se_2CN(i\text{-}Bu)_2)_2PR_3$. A full line-shape analysis of the ^1H NMR spectra of various $Pt(S–S)_2L$ complexes is also consistent with this conclusion.[3b]

The ^{13}C NMR spectra of $Pt(S_2CN(i\text{-}Bu)_2)_2PMe_2Ph$ in $CDCl_3$ (with added CH_2Cl_2 at −70 °C show resonances to be expected from the geometry found in the solid. The dangling dithiolate ligand cis to the phosphine shows no $^{31}P–^{13}C$ coupling while the bidentate ligand displays a $^2J_{C-Pt}$ of 56 Hz. With Pt compounds cis couplings are generally near zero and always much smaller than trans coupling constants.[19]

The result of this work on phosphine adducts of nickel triad 1,1-dithiolates is summarized in Scheme I. Each species now has been identified crystallographically. Exchange rates generally are faster with Pd than with Pt analogues at a given temperature. No five- or six-coordinate species have been isolated with Pd^{II} or Pt^{II} as the metal ions, although a five-coordinate species can be obtained[20] with Ni^{II}. Dynamic NMR data implicate[2a] the formation of five-coordinate species as intermediates with Pd and Pt.

Acknowledgment. The support of NSF Grant CHE-8013141 for structural studies and Grant NIH GM-19050 for dynamical measurements is acknowledged for the work performed at CWRU. The studies at EU benefited from generous loans of K_2PtCl_4 and $PdCl_2$ from Johnson Matthey Ltd. Matthey Bishop, Inc., supplied a generous quantity of $PdCl_2$ for the work at CWRU. The support (to J.M.C.A. and A.J.F.F.) from the SRC also is acknowledged. Crystallographic calculations at EU made use of the "X-ray 72" computer programs. The effort of David Briggs to check tables is greatly appreciated.

Registry No. $Pt(S_2CNEt_2)_2PPh_3$, 40545-16-2; $Pd(S_2PPh_2)_2PPh_3$, 29894-52-8; $Pt(S_2P(OEt)_2)_2PPh_3$, 40537-11-9; $[Pd(S_2PPh_2)(PEt_3)_2]S_2PPh_2$, 29894-48-2.

Supplementary Material Available: Tables S-I to S-VIII, listing thermal parameters and structure factors (20 pages). Ordering information is given on any current masthead page.

Contribution from the Department of Chemistry, University of Auckland, Private Bag, Auckland, New Zealand

Spectroelectrochemistry of Nickel Complexes. Voltammetric and ESR Studies of the Redox Reactions of Phosphine–Dithiolate and Phosphine–Catecholate Complexes of Nickel

G. A. BOWMAKER,* P. D. W. BOYD, and G. K. CAMPBELL

Received October 27, 1981

The redox properties of nickel(II) complexes of the type $[Ni(PPh_3)_2L]^{n+}$ (L = dithiolate (n = 0) or dithiocarbamate (n = 1)) and Ni(dpe)L (dpe = bis(diphenylphosphino)ethane, L = dithiolate or catecholate) have been studied by cyclic voltammetry at a platinum electrode, and the products of the redox reactions have been identified by electron spin resonance spectroscopy. All of these complexes show reversible or quasi-reversible one-electron reduction processes, and the reduction potentials for the PPh_3 complexes are about 0.5 V higher than those of the corresponding dpe complexes. In the case of triphenylphosphine complexes such as $Ni(PPh_3)_2((CN)_2C_2S_2)$, the voltammetry shows evidence of a dissociation equilibrium involving loss of triphenylphosphine from the nickel species present after the electron-transfer process. The frozen-solution ESR spectra of the reduction products show large, anisotropic hyperfine coupling to two equivalent ^{31}P nuclei and anisotropic g values characteristic of d^9 nickel(I) species. The PPh_3 complexes have smaller ^{31}P hyperfine coupling constants than the corresponding dpe complexes. The ^{31}P hyperfine coupling parameters have been analyzed for some representative complexes, and the amount of spin density transferred from the metal to the phosphine ligands has been estimated. In addition to the reduction process, the catecholate complexes undergo a reversible one-electron oxidation. The ESR spectra of the products of such oxidations show only a small ^{31}P hyperfine coupling, hyperfine coupling to nuclei in the catecholate ligand, and almost isotropic g values. These species are therefore formulated as nickel(II) complexes containing coordinated semiquinone radical anions.

Introduction

Transition-metal dithiolene complexes have been the subject of a considerable amount of research over the past 20 years, and several reviews dealing with the unusual chemical and physical properties of these complexes have been published.[1–5] One of the most interesting properties of these compounds is their ability to undergo facile electron-transfer reactions, and

(1) McCleverty, J. A. *Prog. Inorg. Chem.* **1968**, *10*, 49.
(2) Schrauzer, G. N. *Acc. Chem. Res.* **1969**, *2*, 72.

0020-1669/82/1321-2403$01.25/0